NURETH14-200

ANALYSES OF LARGE SCALE TESTS ADDRESSING THE PERFORMANCE OF A CONTAINMENT COOLER AND ITS EFFECT ON GAS DISTRIBUTION

M. Andreani and G. Mignot

Paul Scherrer Institut, Villigen, Switzerland

Abstract

The performance of containment coolers and their effect on the hydrogen risk in the case of an accident with core overheat is an issue that needs to be addressed by means of simulation tools. Four tests performed in the PANDA facility within the OECD SETH 2 project provide a new database to evaluate the capability of the codes to predict the cooling effectiveness of a cooler and its effect on flow patterns and light gas distribution. All tests have been simulated with the GOTHIC code using a three-dimensional mesh and a rather detailed model for the cooler tube bundle. In general, the results obtained are in reasonable agreement with the data, although some major discrepancies have also been observed, which are mostly due to the limited detail permitted by the relatively coarse mesh adopted for all tests of the SETH 2 project.

Introduction

Various plant designs include containment coolers, which are installed in the reactor building to remove the heat during normal operation and may also be used to condense steam in accident conditions. Their use during a severe accident involving release of large quantities of hydrogen raises the question of the effect of the condensation on the distribution of gases and therefore on the role they can play in mitigating or enhancing the hydrogen risk.

The computer codes used for containment analyses must be able to simulate the heat removal capability of these components for the various operating conditions, to represent the effect of their location within the building, to calculate the performance degradation due to non-condensable gases, and to account for the effect of the cooler on gas distribution in a multi-compartment geometry. It is therefore necessary to assess the capabilities of the codes against data from separate-effect tests in a multi-compartment geometry, which include the three-dimensional distribution of gases and steam.

Data in the literature are rather scanty, and do not include the detailed information that is necessary for the assessment of CFD codes, which are increasingly used for containment safety analyses [1]. Four tests performed in the PANDA facility within the OECD SETH 2 project [2] provide a new database to evaluate the cooling effectiveness of a cooler and its effect on flow patterns and light gas distribution [3, 4]. These tests address various combinations of geometry, position and boundary conditions. Due to the main motivation for the tests, i.e. to provide a database for advanced code validation, no scaling criterion has been applied for the selection of the power of the cooler. The heat removal capability of the component has been chosen on the base of the requirements that the power extracted would be much larger than the heat losses and sufficient to condense all injected steam under the condition of slowly increasing pressure (which was investigated in one test).

All tests have been simulated with the GOTHIC code [5] using a three-dimensional mesh and a rather detailed model for the cooler tube bundle. The total number of cells used in the model is about 40'000. The nodalisation is therefore rather fine, but still much coarser than one which would be typically used for a genuine CFD simulation. One of the main interests of this work, however, was to assess the possibility to capture the main trends using a coarse-mesh, similar to that which was successful in predicting basic experiments characterized by stratification build-up [6, 7]. In this paper, only the two experiments addressing the effect of the cooler position will be discussed in some detail, whereas reference to the results for the other two tests will occasionally be made whenever some conclusions are supported by the analyses of the other conditions investigated.

Due to the confidentiality of the data, the simulation results will be displayed together with experimental results on plots without scales. This will not prevent to discuss the quality of the results and to arrive at certain conclusions related to the difficulties to simulate the complex phenomena associated with the operation of a cooler.

1. The PANDA facility and description of the tests

The PANDA facility (Fig. 1, left) mainly consists of six thermally insulated stainless steel vessels. The tests used only the two upper vessels (connected by a large, bent pipe), each of them having a diameter of 4 m and a height of 8 m. For these tests, fluid is injected from a pipe close to the wall in Vessel 1. A water-cooled heat exchanger (cooler) was mounted at two different elevations in the vessel (Vessel 1). Figure 1 (right) shows the two positions of the cooler investigated in this test series.

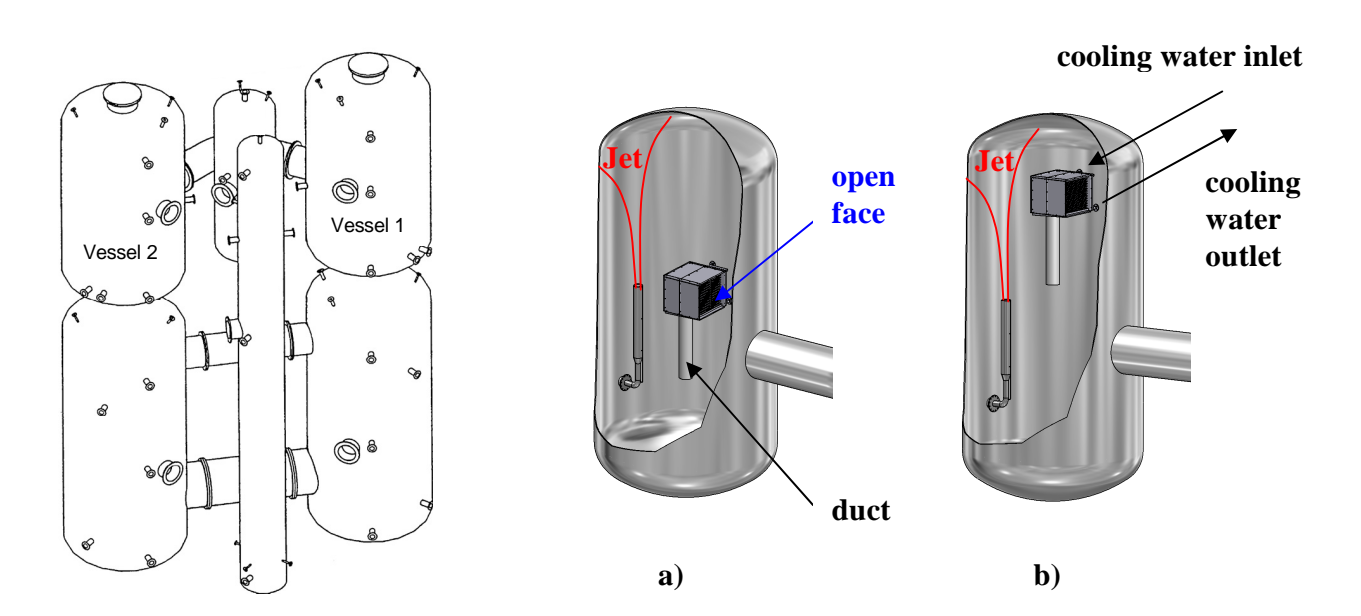


Figure 1 The PANDA facility (left) and the cooler positions in Vessel 1 (right): a), mid-elevation; b) top elevation.

The cooler consists of a case closed on all sides, apart from the face opposite to the interconnecting pipe (Fig. 1), and eight horizontal pipes in a serpentine layout (similar to that of fan coolers), which are connected to inlet and outlet manifolds, where the cooling water is flowing in and out. For three

tests, an exit duct was installed, which is intended to permit the venting of cold gas and therefore to reduce the heat transfer deterioration effect of non-condensable gases and partly stagnating flow. For one test, the duct was removed and the bottom of the case was closed to investigate the effect of the duct. The condensate is drained from the bottom of the cooler case through two pipes (not shown), and flows to the bottom of Vessel 1. Details of the facility and the cooler are given in the companion paper [3].

The PANDA facility [4] is equipped with an extensive standard instrumentation and with a large number of thermocouples, which permit a detailed mapping of the temperature field [4]. Additionally, two mass spectrometers permit the sampling of the mixture composition at 118 sampling points. Due to the duration of the sampling, the number of active lines is chosen for each test with the criterion to obtain the best possible compromise between space and time resolution. Therefore, the information obtained for species concentrations is somewhat coarser than that obtained from the temperature measurement, but very valuable for code assessment. The location of the measurements used for the analyses will be shown together with the results in the following sections. Finally, PIV measurements permitted the observation of the flow in two regions, one above the cooler for the test with cooler at mid-elevation and two below the cooler for the test with the cooler at the top-elevation [3].

All tests included three phases, with initial injection of pure steam during one hour, followed by a release of a mixture of steam and helium during half-an-hour, and finally by the injection of pure steam again. For the first phase the main result is the power extracted by the cooler, whereas for the other two phases the heat transfer degradation due to the light gas, the accumulation of light gas in the cooler and the effect of the cooler on the flow pattern and on the stratification in the two vessels are the principal issues. Three tests were conducted at constant pressure (with a vent from the top of Vessel 2), whereas one experiment was conducted with closed vessels. In this last test (for which the results are not reported in this work), pressure increased during all test phases. The initial conditions (obtained during the pre-conditioning) were prescribed in such a way that condensation could practically occur only inside the condenser. The vessels were thus initially filled with air, and the temperature of the fluid and the structures was initially slightly above the saturation temperature at the total pressure. The injected mixture was somewhat superheated, also with the aim to avoid condensation.

The experiment with the cooler at mid-elevation is identified as Test ST4_2_2 and the experiment with cooler at top elevation is Test ST4_4.

2. The GOTHIC code

GOTHIC [5] is a general-purpose, thermal-hydraulics computer program for design, licensing, safety and operating analysis of Nuclear Power Plant (NPP) containments and other confinement buildings. The thermal-hydraulics module is based on a two-phase, multi-fluid formulation, and solves separate conservation equations for mass, momentum and energy for three fields: a multi-component gas mixture, a continuous liquid, and droplets. In addition, species balances are solved for each component of the gas mixture. GOTHIC includes a full treatment of the momentum transport terms in multi-dimensional models, with optional models for turbulent shear, and for turbulent mass and energy diffusion. The options for turbulence are the mixing-length model and several variants of the k- ϵ model. The hydraulic model of GOTHIC is based on a network of computational volumes (one, two or

three-dimensional) connected by flow paths. In contrast to standard CFD packages, in GOTHIC the subdivision of a volume into a multi-dimensional grid is based on orthogonal co-ordinates. The actual geometry of volumes with curved surfaces (e.g., a cylindrical vessel) can be represented, however, by blocking groups of cells. The numerical solution of the transport equations is based on a semi-implicit method. The method is first-order in time, whereas for the space-discretisation of the advection term both a first-order upwind and a bounded second-order method are available. The 3-D capabilities of GOTHIC, to simulate basic flows of interest for containment analysis, have been extensively investigated (e.g., [6, 7]), and many of the applications to containment analysis include 3-D models. In principle, the code has built-in models for the simulation of condensers, but the heat exchanger component can only be located on flow paths connecting two volumes, and is therefore not suited to simulate in-vessel condensers. Therefore, the choice was made to try to explicitly model the cooler, representing the tubes of the bundle. The version of the code used in the present analysis is GOTHIC 7.2b.

3. Nodalisation and models used for the simulations

The schematic of the model used for the simulations is shown in Fig. 2 for the test with cooler at midelevation (ST4_2_2). The model for test ST4_4 is exactly the same, apart from the cooler (volumes 3, 4 and 5s), which is moved at higher position. The two interconnected vessels are represented with three subdivided volumes (1s, 2s and 3s), connected by 3-D flow connectors.

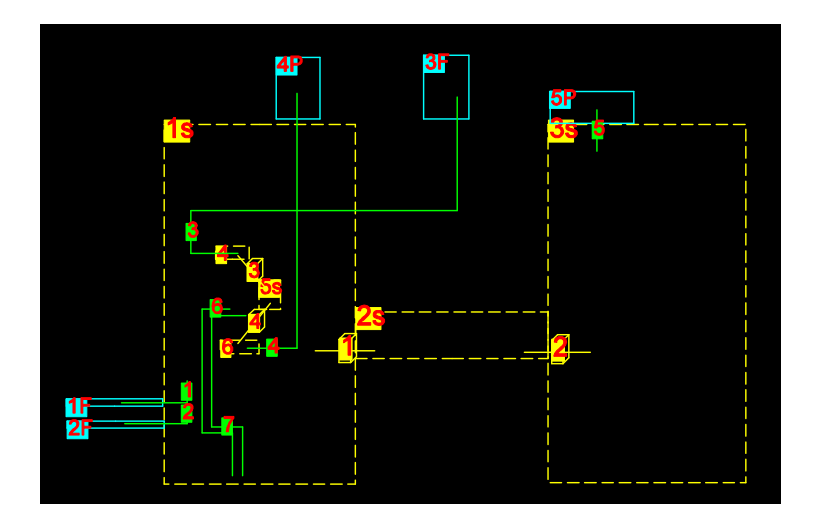


Figure 2 Schematic of the model used for the simulations with GOTHIC.

Steam and helium are separately injected at the bottom of the inlet pipe (modeled as part of Vessel 1, see Fig. 3), and the vent from the top of Vessel 2 permits to keep the pressure constant. The secondary side of the cooler (inside tubes) is represented by an inlet and an outlet volume (Vol. 3 and 4, respectively), which are connected to a subdivided volume (5s) representing the 8-tubes bundle. Figure 3 shows the nodalisation of Vessel 1 and of the cooler (secondary side), which includes the representation of the eight tubes. Blockages in the cells of Vessel 1 permit to represent the injection pipe, the cooler case and the exit duct. The total number of cells used for Vessel 1 (slightly different for the two cases) is about 30'000. The volume of Vessel 1 occupied by the tubes is represented by a porous region. The fluid cells in that region are thermally connected with the fluid inside the cooler through distributed thermal conductors. The cooler tubes are represented by partitioning the volume in

8 unconnected vertical slices. Horizontal partitions between the 8 levels provide an approximation of the "serpentine" flow path within each slice. The 8 tubes are thus represented separately (one tube being marked in Fig. 3 by the blue box). For each tube the heat transfer area is distributed over eight vertical levels. The model for the cooler tubes includes 448 cells. The nodalisation of Vessel 2 (not shown) includes approximately the same number of vertical subdivisions and a much coarser nodalisation of the cross-sectional area. The total number of cells for Vessel 2 is somewhat larger than 9'000. The total number of cells used in the model is thus about 40'000. This model will be referred to as "reference model". The water feed line has not been represented, and the experimental water temperature at the condenser inlet has been used in the boundary conditions.

The standard GOTHIC models have been used for mass and heat transfer (and condensation), and the high-Reynolds number k-ɛ model has been used to represent turbulence. A natural convection correlation for horizontal pipes has been selected for heat transfer on the outside of the cooler tubes. The second-order method in space has been used. Although the models for condensation available in GOTHIC are best suited for heat transfer between the fluid and the structures of a containment and do not provide special features to account for the complex phenomena occurring inside a tube bundle (e.g. formation of liquid bridges, distribution of liquid film around the tube periphery, interaction between tubes, effect of transversal velocity, etc.) this exploratory study was aimed to investigate the possibility to obtain reasonable results using basic models and a coarse mesh. Therefore, no attempts have been made to adjust the models to the specific conditions of the cooler (e.g., using enhancement factors for the condensation heat transfer). Studies on the effect of the condensation models will be performed in the future.

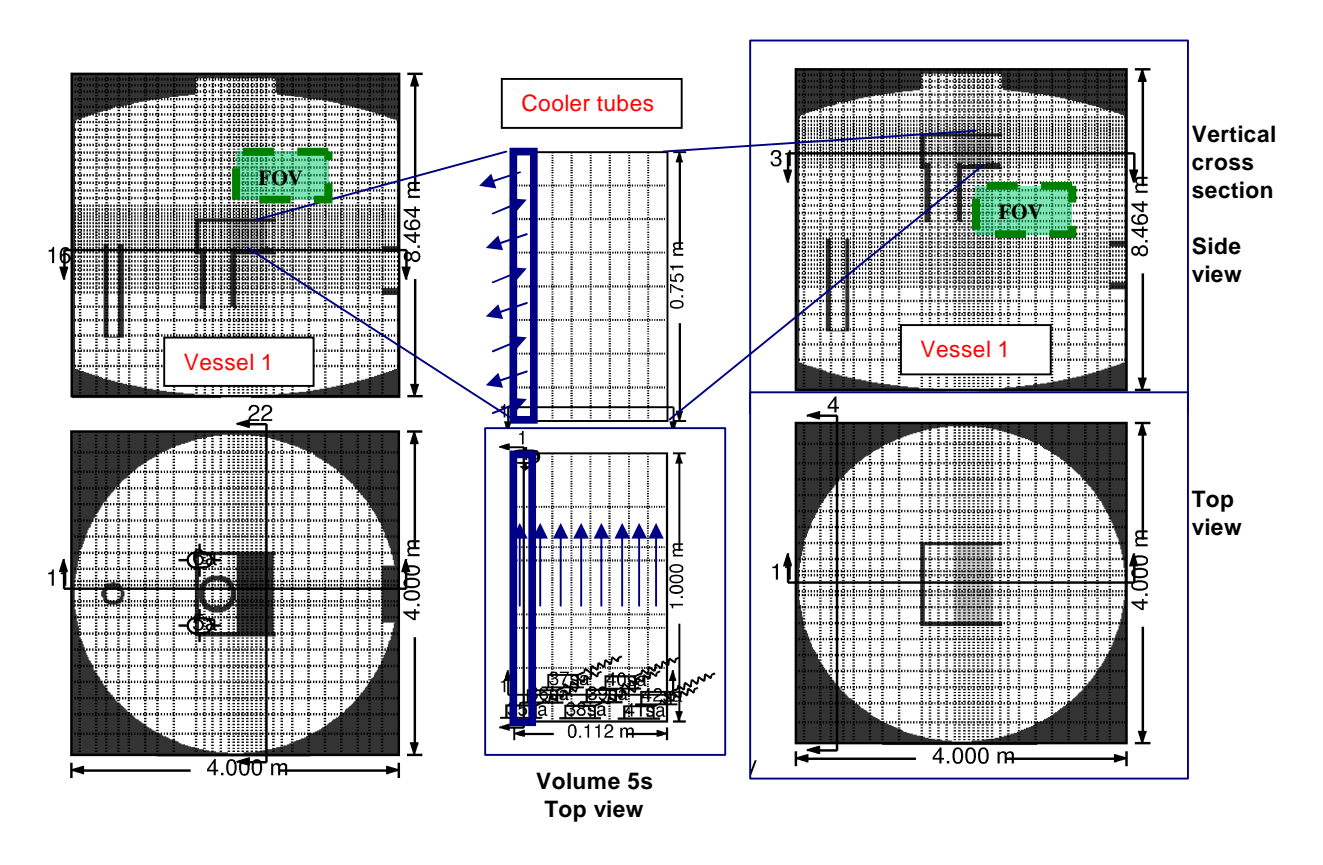


Figure 3 Nodalisation of Vessel 1 and cooler tubes for the two different cooler positions.

4. Results for test ST4_2_2

The comparison of the simulations with the experiments mostly uses fluid temperatures, and helium and steam concentrations. These analyses are complemented by sparse comparisons of the calculated velocity magnitude and direction with the vector fields measured by the PIV in the Field of View (FOV) above the cooler [3]. The positions of the FOV for the two tests are shown Fig. 3.

4.1 Global performance

Figure 4a shows the power extracted by the cooler and the temperatures at the outlet of seven of the tubes (the eighth one was not instrumented, [4]). The code predicts the power fairly well during the initial phase of the test, when only superheated steam was injected. Initially, the prediction is practically equal to the measured power, and in the second half of phase I the calculated heat transfer rate is somewhat overpredicted, but still quite close to the data. This discrepancy will be discussed in section 5, where the power will be compared with that in Test ST4_4. In phase II, the simulation is still reasonably accurate. Especially noteworthy is the correct prediction of the time of the power recovery (at ~ 4800 s) after the temporary reduction. However, the heat transfer deterioration due to the accumulation of helium is underpredicted, and the temporary power surge (above the level before the beginning of helium injection) is not reproduced. The simulation of the power history in Phase III, when only steam is again injected, on the other hand, is poorly predicted. Whereas in the experiment the power was practically constant, the simulation shows a continuous degradation, accompanied by a large oscillation. These results can be interpreted using the information on gas concentrations, as discussed in the next section. It is worth mentioning here, however, that also for the other tests with cooler at mid-elevation position the prediction of Phase III was rather unsuccessful.

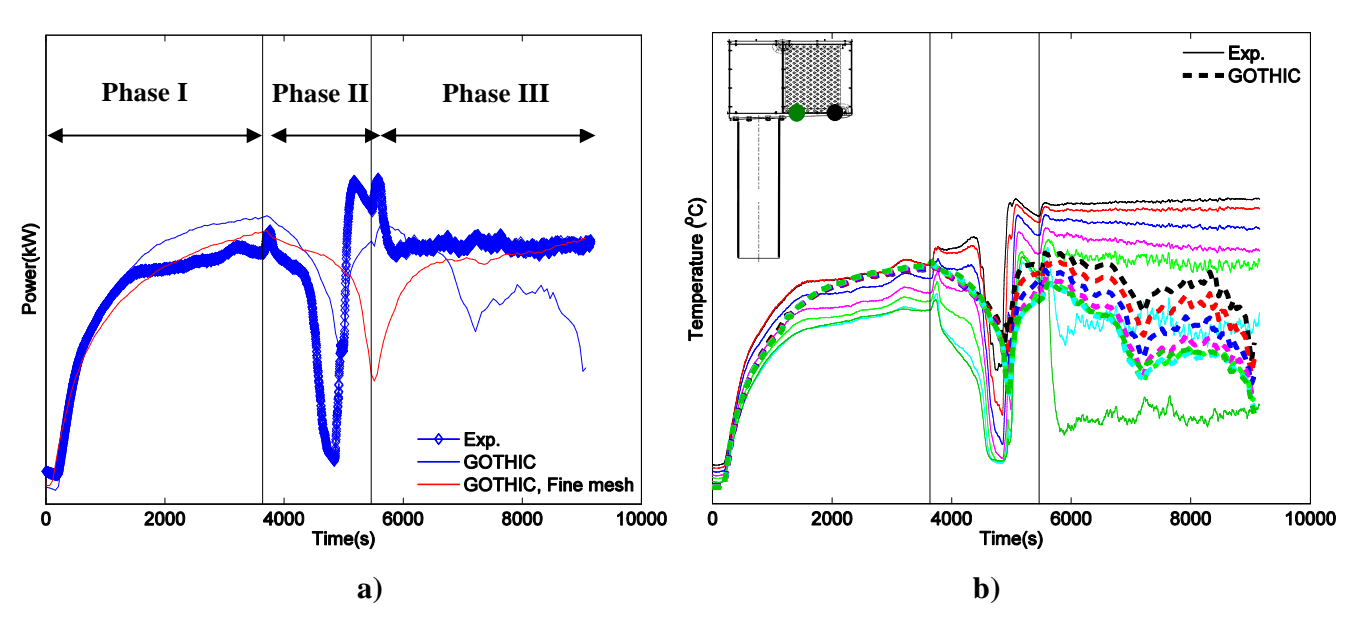


Figure 4 Test ST4_2_2: Cooler power (a) and water temperatures at the outlet of the pipes (b).

Figure 4b shows the water temperatures at the outlet of the seven instrumented pipes. For clarity, in the diagram showing the schematic of the cooler, only the positions of the measurements in the front tube and the tube close to the empty space are shown in black and dark green, respectively. It can be observed that the thermal load of the various tubes was quite different in the experiment, with the tube

in front (close to the open face) taking the largest power, and the tubes close to the empty space behind the bundle becoming nearly inactive in Phase III. The calculation, however, predicted nearly the same temperature rise in all tubes during Phases I and II, and too little difference between the tubes during Phase III. Although these differences could partly be due to the inhomogeneous distribution of the water flow inside the tubes, it is more likely that the differences are mostly produced by the large inhomogeneities in the gas mixture composition on the primary side (see next section). It should be remarked that the global power during the first two phases was little affected by the large discrepancy in the distribution of thermal load of the pipes, whereas this deviation is probably the cause (or the most striking result) of the large deviations in Phase III.

Figure 4a also shows the results of a calculation using a refined mesh of the cooler, where the number of subdivisions of the zone of the cooler was increased to 16 in both vertical and transversal direction. For this calculation, however, only one vessel was represented and a coarser mesh for the subdivision of the vessel had to be used to keep the calculation time within reasonable limits. The vertical subdivision of the zone where the cooler is located, however, was also finer (16). The representation of one vessel is clearly a severe limitation of this second model (referred to as "fine-mesh model), but this study was only performed to try to understand to what extent the discrepancies observed in the simulation with the reference model (especially for Phase I) could be due to the coarse mesh and to the flow blockage in the duct.

The fine-mesh representation of the cooler clearly produced different results, with delayed power recovery (at the end of the helium injection) and higher (and nearly constant) power in phase III. The tube outlet temperatures (slightly lower) were again very close to each other. These results are discussed in the section 4.4, where these effects will be correlated to the calculated flow patterns. The lower power during phase I is due to the lower steam fraction at the inlet of the cooler, due to the numerical dilution of the jet caused by the coarse mesh in the region outside the cooler. This result shows that a sufficiently fine mesh is required not only for the representation of the cooler but also for the entire flow domain.

4.2 Gas distributions inside and around the cooler

The overprediction of power extracted during Phase I and part of Phase II could be due to either too large transport of steam to the cooler or inaccurate representation of flow and heat transfer inside the cooler. As the steam concentration above the cooler was well predicted, it can be assumed that the propagation of steam towards the cooler was well represented. Since, however, the calculated velocities in the FOV of the PIV were about the half of the measured values, it can be argued that the jet momentum (as expected) was dissipated too much along the flow loop generated by the injection. The effect of this discrepancy on the cooler performance, however, is difficult to estimate. The distribution of steam within the cooler can be analysed to obtain some information on the processes inside the cooler. Figure 5 shows the steam concentrations measured at the bottom of the duct and inside the cooler. It is clear that the large inhomogeneities in both vertical and transversal directions measured in the experiments were not reproduced by the code, which only reproduced to some extent the vertical stratification. The calculation with the finer mesh also could not predict the low steam concentrations in the lower part of the cooler. This could be due to the coarse mesh used for representing the bundle, which promoted mixing, or to the inability of the condensation model to account for the complex conditions prevailing in a tube bundle (e.g., formation of liquid bridges, distribution of liquid film

thickness along the tubes, etc.). The coincidence in time (at ~ 1500 s) between the deviation of the power (Fig. 4a) and the start of the discrepancy in the steam concentration at the duct exit and in the rear part of the cooler (black and red curves in Fig. 5, respectively) could suggest that the inaccuracy in the predictions could also be due to a change in the flow through the duct (or, conversely, this could be the effect rather than the cause of the wrong prediction of the gas mixture composition, and therefore density, distribution within the cooler). Indeed (see next section), the reference calculation predicted the flow through the duct to terminate at around 1600 s, whereas the temperature measurements [3] indicate that the flow continued through Phase I. The simulation with the finer mesh, however, predicted a continuing flow through the duct, but could not reproduce the experimentally observed change in power increasing rate, which is clearly correlated with the termination of steam concentration increase in the middle of the empty space (red curve). Moreover, as similar results (and deviations) have been observed for the test where the duct was removed, it can be argued that the capability of the code to calculate the cooler power during the steam injection phase is practically unaffected by the simulation of the flow through the duct, but is controlled by the calculation of the gas distribution within the bundle. The distribution of helium inside the cooler and immediately above it is shown in Fig. 6. The process of accumulation inside the cooler during phase II is reasonably well predicted by the code, which also represents correctly the vertical distribution. Alike for steam, however, the calculated helium concentration in the empty zone behind the tubes is largely deviating from the measurements, which indicates a difficulty to represent some features of the flow circulation inside the cooler. It is interesting to note that the helium concentration sudden drop in the lower part of the cooler at around 5000 s and the faster rise above the cooler shortly afterwards could be predicted. This event, which is due to the change in global flow pattern (see next section), could be captured by the code.

4.3 Flow patterns

Figure 7 shows the temperature distribution and the gas velocity vectors in a vertical plane bisecting the cooler and including the axis of the vessel and the interconnecting pipe. At the beginning of the steam injection phase (see Fig. 7a, at t=500 s), the fluid in the cooler is strongly cooled by condensation in the tubes, and falls through the duct. Still during phase I, after 1500 s (Fig. 7 b), this flow is blocked. In the experiment, however, the flow through the duct terminated at the beginning of Phase II. A second deviation from the experiment is that a portion of the cold fluid spilled over the edge of the cooler from the open face and created a falling, negatively buoyant plume. This second flow path of the cold fluid was not observed in the experiment [3]. These two discrepancies, which are due to a different density distribution inside the cooler, were probably caused by large deviations in the distribution of condensation rates and mixing inside the cooler. As the fine-mesh calculation did predict continuing flow through the duct and still could not predict the distribution of steam inside the cooler and the different load of the tubes, it can be concluded that the flow through the duct did not play a major role.

During phase II, the helium accumulated inside the cooler, because of the recirculating flow, which prevented the helium to escape from the zone of the bundle, and caused a decrease in the heat transfer rate. Figure 7c) shows this situation at the time of the largest power degradation. When the helium concentrations became sufficiently high and the cold mixture became lighter than the fluid above, the flow pattern changed dramatically (Fig. 7d). Shortly after 5000 s, the helium-rich mixture started to flow out of the cooler through the top of the case, creating a narrow, rising plume. This event can be associated with the power recovery and helium concentration increase above the cooler (see previous sections), although the power recovery has probably started few hundreds seconds earlier due to

internal flow re-arrangement inside the cooler. [4]. The velocity field measured by the PIV [3, 4] also confirmed the presence of a rising plume above the cooler. The calculated plume is weaker than in the experiment because the helium concentration in the mixture emerging from the cooler is lower (and the mixture density higher) than in reality. This is probably the main reason why this flow pattern is not stable, as it can be recognized in figures 7c) to 7e). These three snapshots show the flow transitions which produce the large oscillation, which appears in the power history (Fig. 5). In fact, after the period of flow confinement (Fig. 7c) and an initial period following the formation of a rising plume (Fig. 7d), this flow structure (Fig. 7e) disappears and the flow is confined again within the cooler. After the helium concentration increases again, the fluid inside the cooler becomes lighter again, and a weak plume is re-established for a while (Fig. 7f). The final power decrease is associated with the confinement of the flow inside the cooler case, with disappearance of the rising plume. In the simulation with the fine mesh for the cooler, however, the rising plume is stable and the power history in the later portion of phase III becomes very close to the experimental one.

Figure 7 also shows a flow from the top of the IP towards the open face of the cooler. As this flow from Vessel 2 carries an air-rich mixture, its influence on the cooler behaviour could be important. However, as from the experimental information it is not possible to infer whether such a flow existed or not, this aspect, which strongly complicates the analysis of the results, has not been considered in this work.

In summary, different aspects of the phenomena prevailing in the cooler could be captured by the two meshes, but it was not possible to reproduce the correct behaviour entirely with any of them. As simulations with an even finer mesh for the entire flow domain cannot be afforded, it is not possible at present to draw conclusions with respect to the capabilities of the code to represent the thermal-hydraulic behaviour of the cooler and its effect on the gas distribution

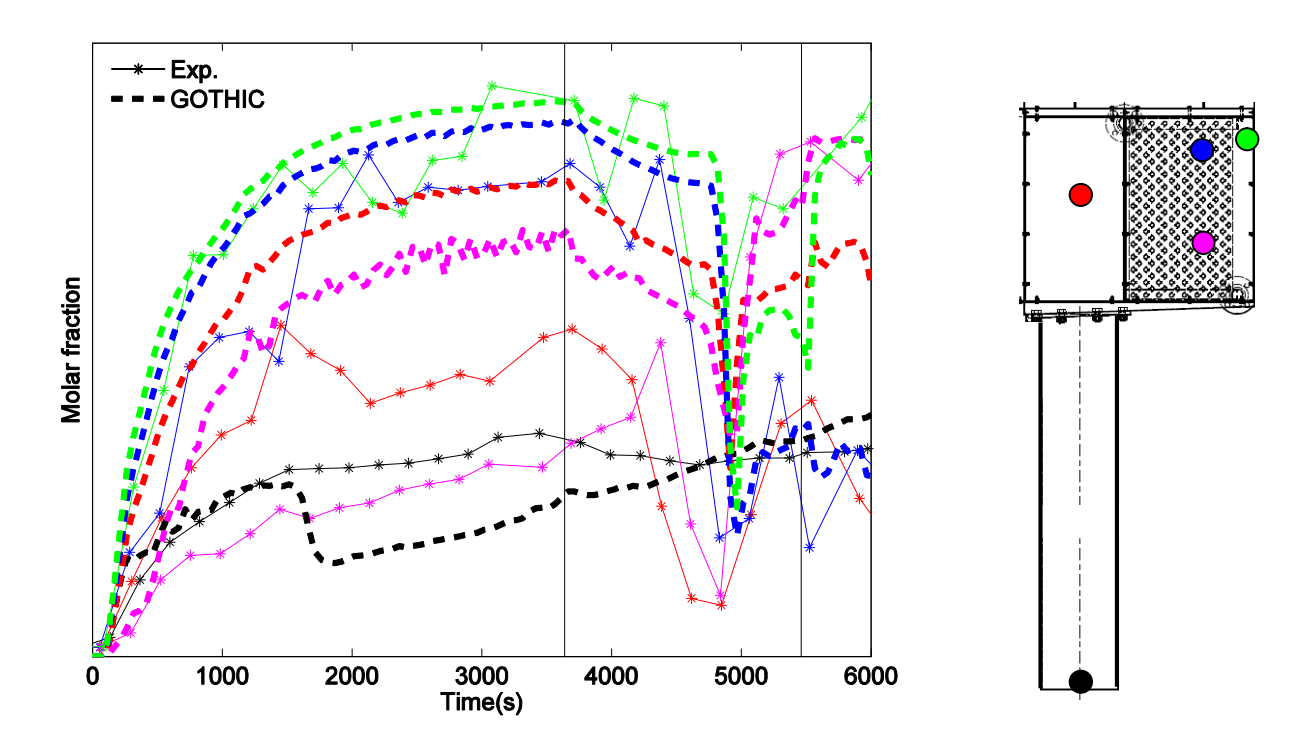


Figure 5 Steam concentrations inside the cooler.

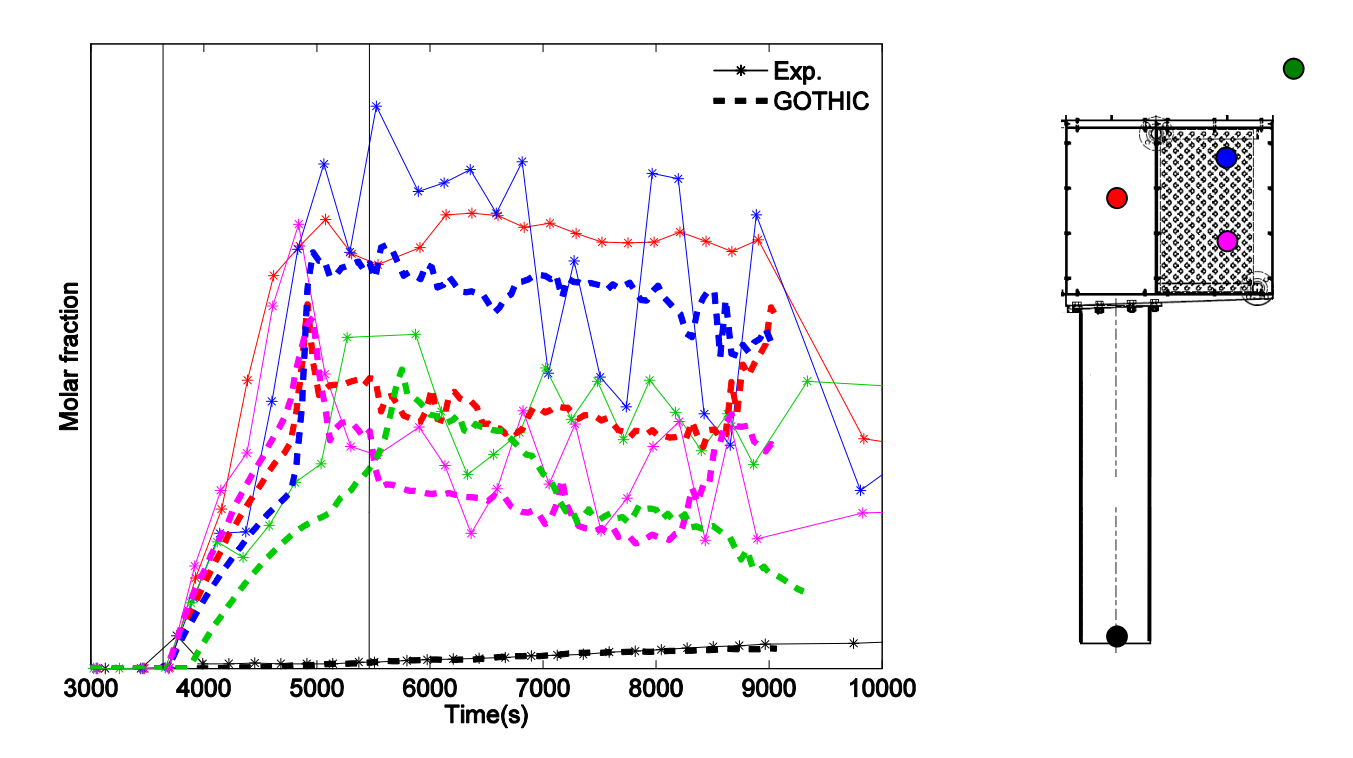


Figure 6 Helium concentrations inside the cooler and immediately above it.

4.4 Effect of cooler on the gas distribution in Vessel 1 and transport into the adjacent vessel

In the previous sections, the comparison between the calculated and the experimental thermal-hydraulic behaviour of the cooler has been presented. In this section, the capability of the code to represent the effect of the cooler on the ambient is discussed. Figure 8 shows the steam and helium concentrations along the axis of Vessel 1 for selected elevations.

During Phases I and II the distribution of steam is calculated fairly well. The steam fractions at the highest elevations, however, are overpredicted at the onset of the helium-rich plume rising from the cooler (see above). Moreover, the steam concentration at the bottom of the vessel shows noticeable deviations, which originate from the incorrect timing of the flow blockage in the duct.

In Phase II, also the helium concentration can be considered to have been reasonably well predicted, although the accumulation at the top of the vessel could not be reproduced due to the underprediction of the strength of the plume rising from the cooler. The predictions for Phase III are rather poor, as it could be expected from the incapability of the model to correctly represent the helium-rich plume escaping the cooler starting from the end of phase II. Finally, the distributions of steam and helium in Vessel 2 are shown in Fig. 9. The steam and helium transport during Phase III are both overpredicted, as expected from the lower accumulation in Vessel 1. These discrepancies are probably that most concerning in relation to the applicability of coarse-mesh methods to safety analyses, because in previous investigations without cooler [6] the transport of gas in the vessel adjacent to that of the

injection could be calculated accurately using a coarse mesh. The present results show, however, that the presence of a cooler (condenser) is likely to pose severe problems for the simulation of the distribution of gases within a compartmented geometry.

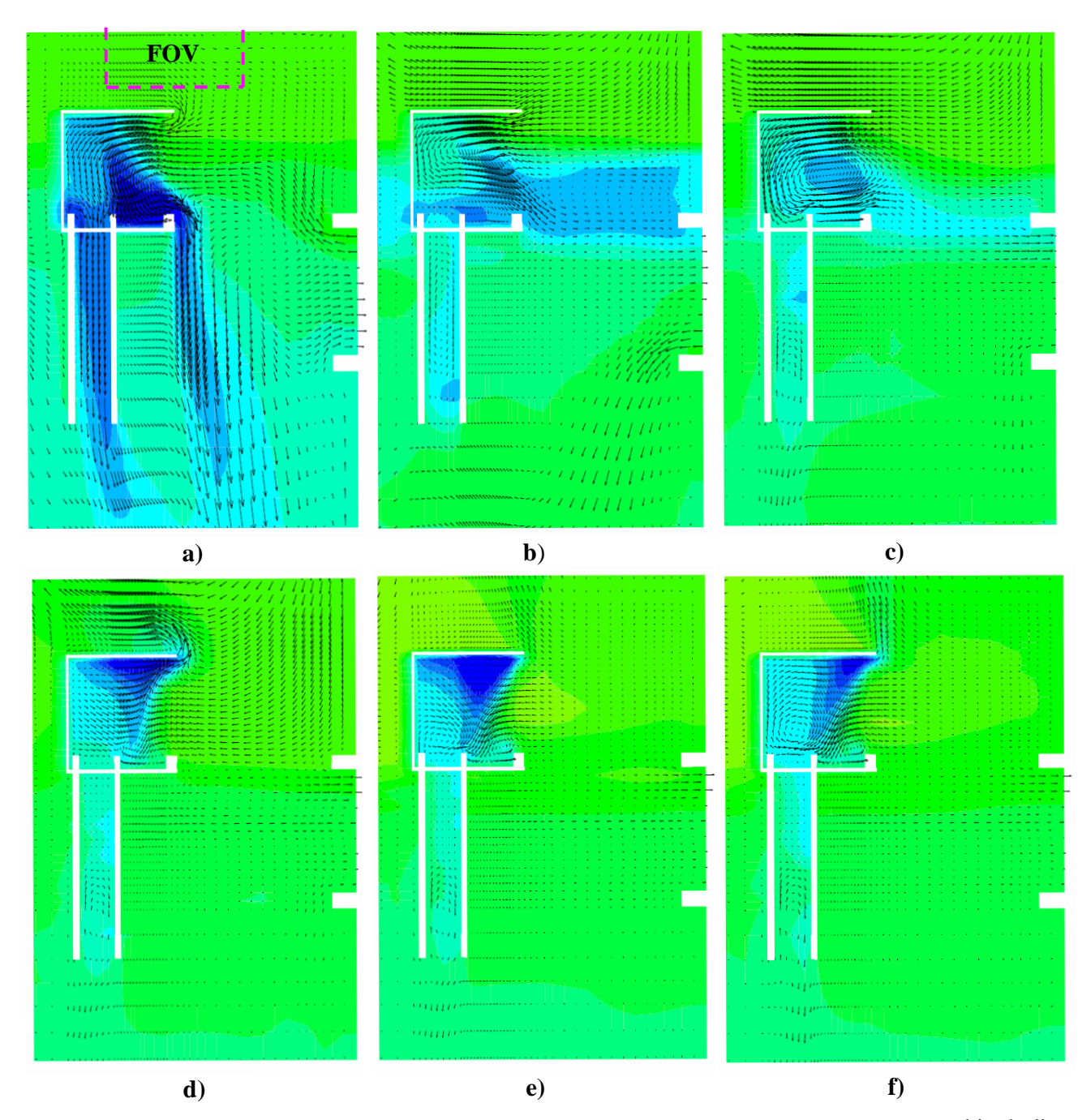


Figure 7 Temperature distribution and gas velocity in the vertical plane cutting the cooler and including the vessel axis: a) t=500 s; b) t=1500 s; c) t=5000 s; d) t=5400 s; e) t=7300 s; f) t=8100 s. The temperatures scale goes from blue (cold) to green (warm).

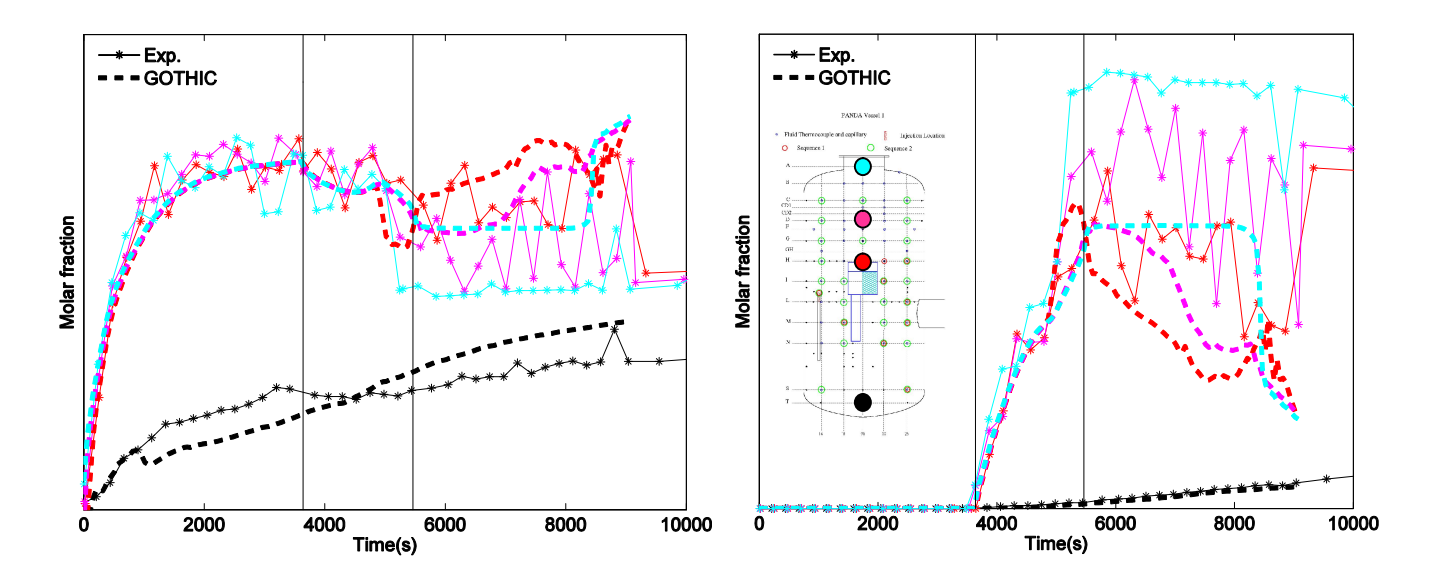


Figure 8 Gas distributions along axis of Vessel 1: a) steam; b) helium.

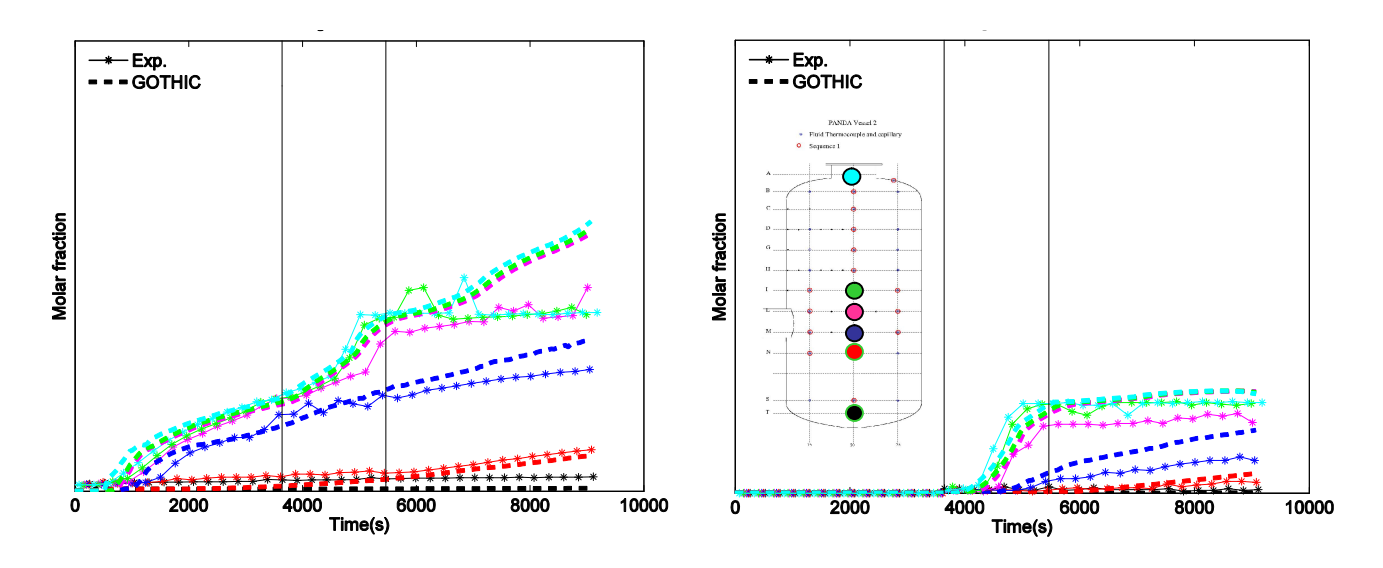


Figure 9 Gas distributions along axis of Vessel 2: a) steam; b) helium

5. Results for Test ST4_4

In this section, due to space limitations, only selected results are reported, focusing on the possible explanation for the differences with respect to Test ST4_2_2.

5.1 Cooler performance and gas distributions

In the configuration of Test ST4_4, the ambient fluid above the injection remains longer a steam-lean mixture (due to the condensation above) so that the injected fluid arrives more diluted in the dome of the vessel. This results in a lower steam fraction in the mixture entering the cooler. Intuitive considerations would suggest that the power exchanged by a cooler in the higher position should be

thus smaller than with the condenser at lower elevation, because the lower steam fraction (larger amount of non-condensable gases) is expected to produce lower condensation rates in the cooler. Actually the calculated power is smaller for Test ST4_4 than for Test ST4_2_2, but the experiments show an opposite trend. Figure 10 shows that the code, contrarily to the result for Test ST4_2_2, underpredicts the cooler power. The somewhat unexpected experimental behaviour can be caused by various reasons, and it is not speculated here which effect is the controlling one.

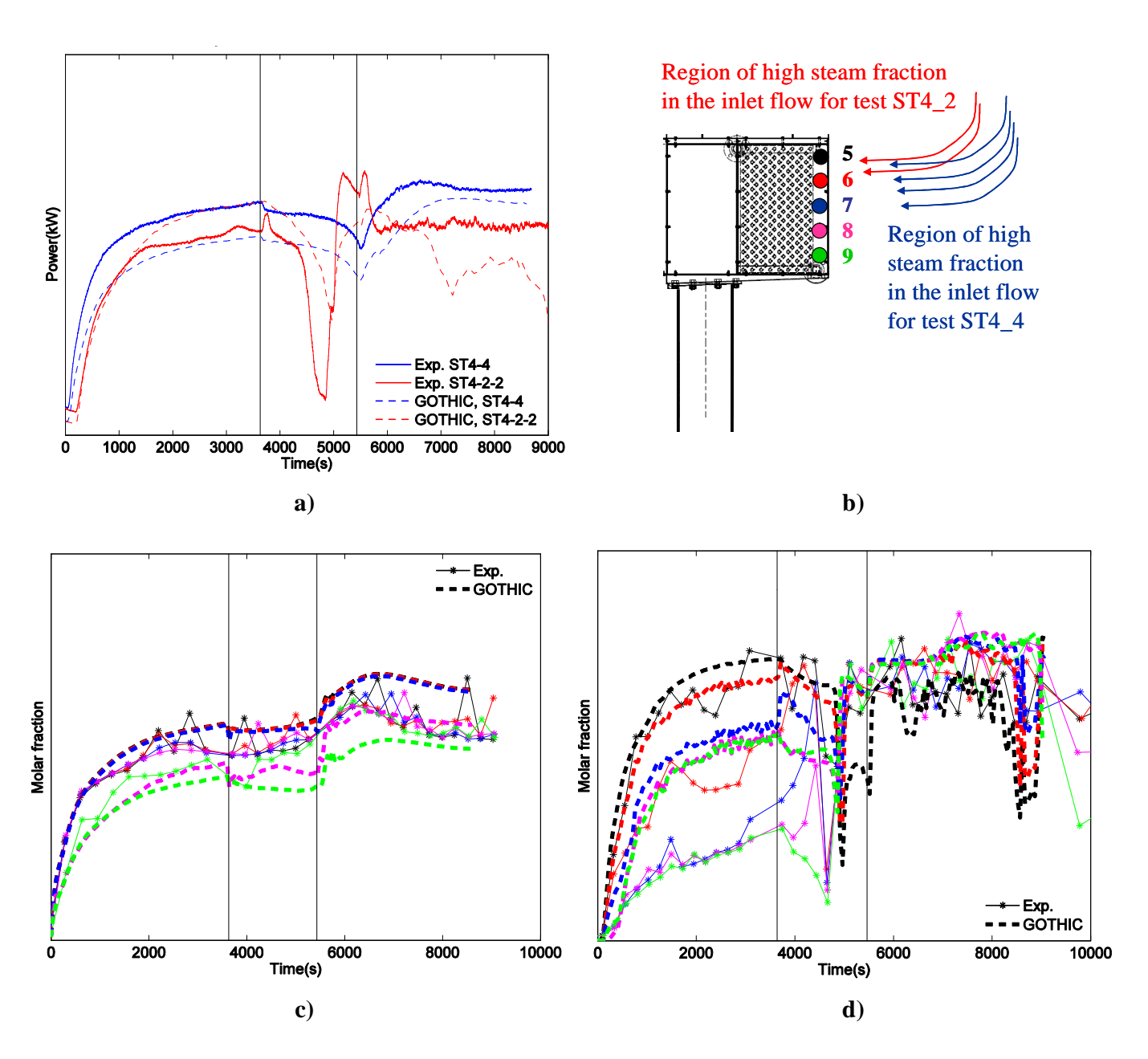


Figure 10 Comparison of simulations and experiments for tests ST4_4 and ST4_2_2: a) cooler power; b) sketch of the expected inlet flow and positions of the sampling points; c) steam fraction distribution at the open face for test ST4_4; d) Steam fraction distribution at the open face for test ST4_2_2.

As for the simulations, the difference in the global heat exchange rate can be related to the different distribution of steam at the inlet to the cooler. In fact, Figure 11 shows that for Test ST4 2 2 high steam concentrations are calculated over the entire height of the open face, whereas in the test a mixture of high steam content approaches the tubes only over a thin layer (spanning a vertical height not larger than the distance between the two sampling points 5 and 6). The overprediction of the power for test ST4_2_2, therefore, is possibly due to a too large portion of the tube heat transfer area exchanging heat with a high-steam fraction mixture. This effect could have over-compensated too low heat transfer coefficients, which could be expected from neglecting in the models the various enhancement mechanisms present in a bundle (see section 3). For test ST4_4, however, the steam fraction at the inlet to the cooler is smaller, more homogeneously distributed, and close to the experimental values. Assuming that the other inlet conditions (velocity) were similar to those of the experiment, the underprediction of the power would be thus the result of lower "average" condensation heat transfer coefficients. Although the calculated power extracted is lower than the experimental one, the agreement of the simulation with the test for other aspects is remarkable. In particular, the degradation of the heat transfer during the steam/helium injection phase, the time of the recovery (a short time after the termination of the helium injection) and the stabilised cooler power achieved at the end of phase III Similarly to test ST4_2_2, also for this test the large water temperature were all well predicted. differences between the various tubes could not be predicted, confirming the difficulty to simulate with a coarse mesh the strong gradients prevailing inside the cooler.

5.2 Flow patterns

The good agreement in the cooler power history is the result of a generally acceptable representation of the main flow patterns that could be inferred from gas temperatures and concentrations [4] and the limited information for the PIV located below the cooler [3]. Although the times of the transitions and the details of the flow are not precisely reproduced, the main features of the flow patterns were properly simulated. Figure 11 shows four snapshots of the temperature distribution in Vessel 1 and gas velocity fields at various representative times. In general, one recognises that the flow through the duct never stopped, while the flow from the bottom of the cooler became weaker and weaker during Phase 2 (and nearly stopped for few hundreds seconds at around 5400 s), and became stronger again in Phase III. The persistence of this second flow path could not be recognised from the temperature measurements [4] and cannot be confirmed by the PIV measurements [3], because a kind of weak recirculation zone could be observed in the FOV.

5.3 Gas distribution in Vessels 1 and 2

The effect of the cooler at mid-elevation was that to produce a strong and stable stratification in Vessel 1, which could not be reproduced by the code, and a moderate accumulation in Vessel 2 which was simulated, though with large inaccuracy. For test ST4_4, with cooler in a higher position, the simulations also show major discrepancies. In fact, Figure 12 (left) shows that the concentration of helium in Vessel 1 (Phases II and III) is only well predicted in the region above the exit of the duct, which is basically not affected by the cooler, as the outflow from the open face is not the main flow path of the exhaust mixture. However, at elevations immediately below the duct, where the fluid composition is affected by the mixture discharged by the cooler, the measured high concentrations cannot be reproduced, because the helium accumulation inside the cooler (not shown) is underpredicted due to the lower condensation rate. Moreover, the global mixing process that results in the progressive concentration equalisation at all elevations in Vessel 1 could not be predicted. As the helium

concentration in the region of the interconnecting pipe was underpredicted, the amount of helium transported to Vessel 2 is also underpredicted. This resulted (fig. 12, right) in lower helium concentrations in the upper part of Vessel 2.

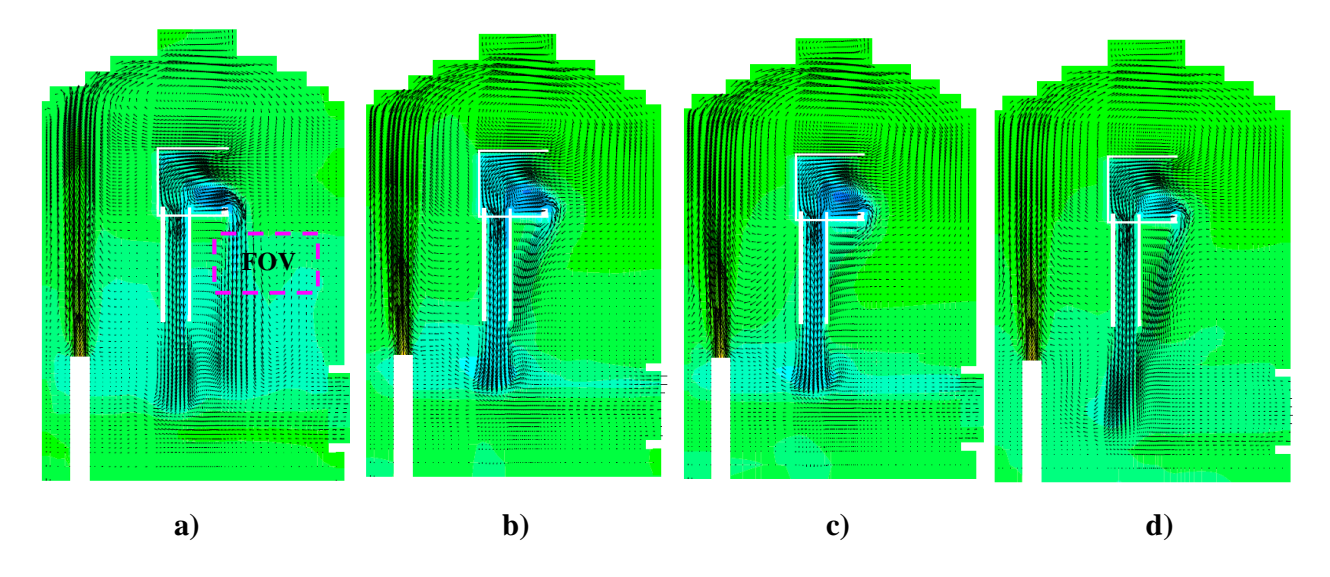


Figure 11 Calculated gas temperature distribution and velocity field in Vessel 1 for test ST4_4: a) t=1500 s; b) t=5100 s; c) t=5400 s; d) t=8800 s.

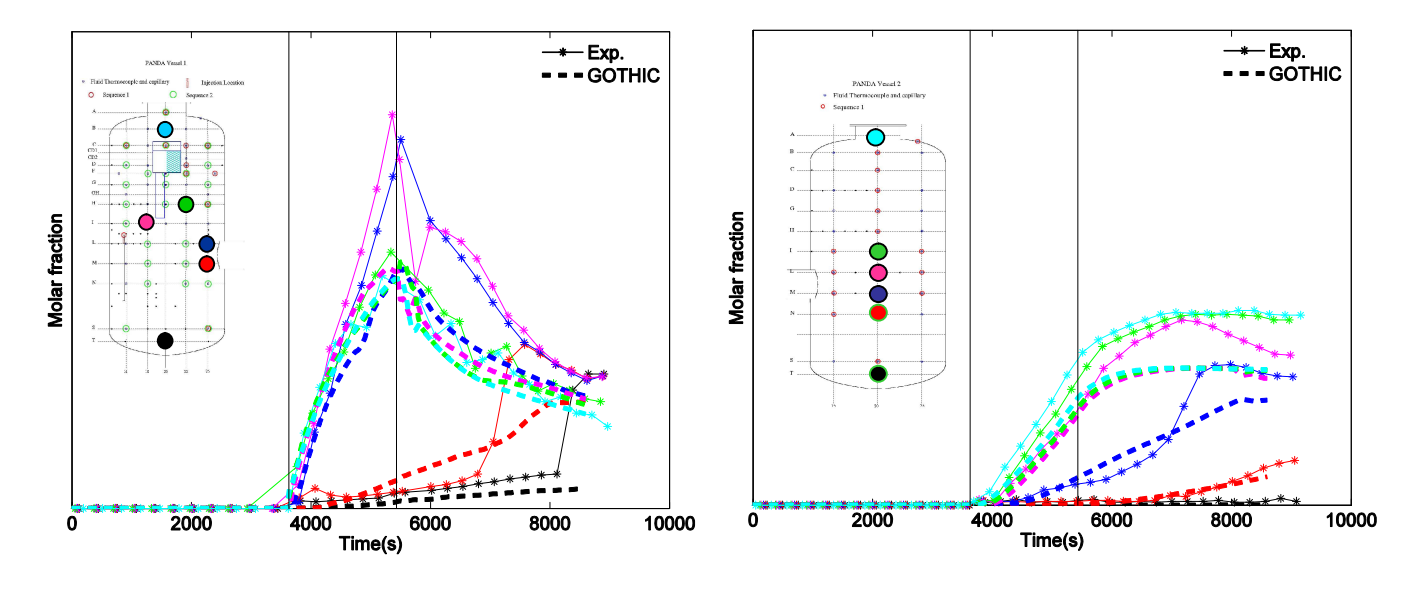


Figure 12 Vertical distribution of helium in Vessel 1 (left) and Vessel 2 (right).

6. Conclusion

The tests in the PANDA facility investigating the performance of a cooler and its effect on light gas mixing have been simulated with the GOTHIC code. This exploratory study included the attempt to

model in detail the geometry of the cooler. In particular in this work the results for the two tests addressing the effect of the vertical position of the cooler have been presented.

In general, the results obtained are in reasonable agreement with the data, although major discrepancies have also been observed. The power was fairly well predicted, but the effect of the cooler position could not be reproduced. The reason for the difficulty was the limited resolution of the coarse mesh adopted, which did not permit to simulate properly the conditions at the inlet of the cooler and inside it. The limited mesh sensitivity analysis (with refinement for the cooler but coarser mesh for the other regions) performed for one of the tests showed that the mesh has a major effect on the results.

For the phase with injection of light gas (helium), the heat transfer degradation due to the accumulation of non-condensables could be captured, at least in a qualitative sense. The concentration of helium inside the cooler, however, was strongly underpredicted, and this resulted in large discrepancies with the experiment for the test with cooler at mid-elevation in phase III, when again only steam was injected. The sensitivity study showed again that some aspects of the phenomena could be recovered using a finer mesh for the cooler, although the simulation degraded with respect of the timing of cooling power recovery. In summary, the main conclusion of the study is that a fine mesh in the entire flow domain is essential for capturing all phenomena that control the accumulation of gases inside the cooler, its effect on its performance and the flow patterns around the cooler generated by the density differences produced by the distribution of gases. In consideration of the observed mesh dependency, investigations on the effect of condensation models were not carried out.

As a consequence of the difficulty to predict the non-condensable build-up inside the cooler and the resulting flow patterns, large discrepancies in the distribution of helium inside the two vessels were observed in the simulations. Indeed, the stable stratification for the test with cooler at mid-elevation and the global mixing in the second test in Vessel 1 could not be predicted, and large inaccuracies in the prediction of the distribution in Vessel 2 were observed.

From this study it has been learned that the simulation of an internal condenser is a very challenging task (much more than initially anticipated), which requires first of all a sufficiently detailed model. Although the difficulties could have been amplified by the specific geometry of the cooler (with a closed case, which permits accumulation of gases), it is clear that the appropriate modelling of a cooler could be very demanding. Investigations with a finer mesh will help clarifying the issue. However, within the scope of the activities accompanying the present project, the use of the nodalisation that was successful for other applications was motivated by the necessity to use a consistent approach for all cases investigated and arrive at an overall assessment of the predictive capabilities of coarse-mesh simulations.

Acknowledgments

The authors gratefully acknowledge the support of all the countries and the international organizations participating in the OECD/NEA SETH-2 project, and particularly of the members of the Management Board and the Programme Review Group of the SETH-2 project.

7. References

- [1] D. Paladino, M. Andreani, R. Zboray, and J. Dreier, "Toward a CFD-quality database addressing LWR containment phenomena", <u>CFD4NRS-3: Experimental Validation and Application of CFD and CMFD codes to Nuclear Reactor Safety Issues</u>, Washington D.C., USA, 2010, September 14-16.
- [2] D. Paladino, M. Huggenberger, M. Andreani, S. Gupta, S. Guentay, J. Dreier, H.M. Prasser, "LWR Containment Safety Research in PANDA", <u>Proceedings of the 2008 International Congress on Advances in Nuclear Power Plants (ICAPP `08)</u>, Paper 8303, Anaheim, CA, USA, 2008, June 8-12.
- [3] R. Kapulla, G. Mignot, D. Paladino, N. Erkan and R. Zboray, "Thermal Hydraulic Phenomena Caused by the Interaction of Steam and Steam-Helium Mixture Wall Jets with a Containment Cooler", <u>Proceedings of the 2011 International Congress on Advances in Nuclear Power Plants (ICAPP `11)</u>, Paper 11093, Nice, France, 2011, May 2-5.
- [4] G. Mignot, R. Kapulla, N. Erkan, R. Zboray and D. Paladino, "Containment cooler performance in the presence of light non condensable gas with cooler location as a primary parameter", this conference, Paper 239.
- [5] GOTHIC Containment Analysis Package, Version 7.2b(QA), EPRI, Palo Alto, CA, March 2009.
- [6] M. Andreani and D. Paladino, "Simulation of gas mixing and transport in a multi-compartment geometry using the GOTHIC containment code and relatively coarse meshes", Nuclear Eng. Design, 240, 1506-1527 (2010).
- [7] M. Andreani, T. George and D. Paladino "Simulation of basic gas mixing tests with condensation in the PANDA facility using the GOTHIC code", Nuclear Eng. Design, 210, 1528-1547 (2010).